Chinese Journal of Polymer Science Vol. 30, No. 6, (2012), 853–864

Chinese Journal of Polymer Science

TOUGHENING OF ETHYLENE-PROPYLENE RANDOM COPOLYMER/CLAY NANOCOMPOSITES: COMPARISON OF DIFFERENT COMPATIBILIZERS*

Bin-bin Liu[a], Yong-gang Shangguan[a] and Qiang Zheng[a, b**]
[a] *Key Laboratory of Macromolecular Synthesis and Functionalization of Ministry of Education, Zhejiang University, Hangzhou 310027, China*
[b] *Department of Polymer Science and Engineering, Zhejiang University, Hangzhou 310027, China*

Abstract Ethylene/propylene-random-copolymer (PPR)/clay nanocomposites were prepared by two-stage melt blending. Four types of compatibilizers, including an ethylene-octene copolymer grafted maleic anhydride (POE-*g*-MA) and three maleic-anhydride-grafted polypropylenes (PP-*g*-MA) with different melt flow indexes (MFI), were used to improve the dispersion of organic clay in matrix. On the other hand, the effects of organic montmorillonite (OMMT) content on the nanocomposite structure in terms of clay dispersion in PPR matrix, thermal behavior and tensile properties were also studied. The X-ray diffraction (XRD) and transmission electron microscopy (TEM) results show that the organic clay layers are mainly intercalated and partially exfoliated in the nanocomposites. Moreover, a PP-*g*-MA compatibilizer (compatibilizer B) having high MFI can greatly increase the interlayer spacing of the clay as compared with other compatibilizers. With the introduction of compatibilizer D (POE-*g*-MA), most of the clays are dispersed into the POE phase, and the shape of the dispersed OMMT appears elliptic, which differs from the strip of PP-*g*-MA. Compared with virgin PPR, the Young's modulus of the nanocomposite evidently increases when a compatibilizer C (PP-*g*-MA) with medium MFI is used. For the nanocomposites with compatibilizer B and C, their crystallinities (X_c) increase as compared with that of the virgin PPR. Furthermore, the increase of OMMT loadings presents little effect on the melt temperature (T_m) of the PPR/OMMT nanocomposites, and slight effect on their crystallization temperature (T_c). Only compatibilizer B can lead to a marked increases in crystallinity and T_c of the nanocomposite when the OMMT content is 2 wt%.

Keywords: Polypropylene; Clay; Compatibilization; Nanocomposites.

INTRODUCTION

Polypropylene (PP) has been used widely in several industrial fields due to its good performances and low price. Since the montmorillonite (MMT) is a kind of mineral with layered structure[1], it could be used to modify PP for improving the barrier property. In general, a no more than 5% MMT addition into PP may decrease the gas diffusion in matrix and enhance the mechanical and thermal properties of the resulting nanocomposites. Hence, PP/MMT nanocomposites have attracted great attention in the past two decades[2–12].

In order to obtain PP/MMT nanocomposites with excellent performances, some important factors have been extensively discussed, including (i) the size of montmorillonite particle, (ii) the space dimension between layers of montmorillonite and (iii) the dispersion of montmorillonite in PP matrix. Usually nano grade is considered to be the best, and the most commonly used nano clay is derived from the Na-montmorillonite,

* This work was supported by the National Basic Research Program of China (No. 2005CB623800), Joint Research Fund for Overseas Chinese Young Scholars (No. 50728302) and the Program for Zhejiang Provincial Innovative Research Team (No. 2009R50004).
** Corresponding author: Qiang Zheng (郑强), E-mail: zhengqiang@zju.edu.cn
Received February 7, 2012; Revised April 17, 2012; Accepted April 23, 2012
doi: 10.1007/s10118-012-1185-4

whose average interlayer spacing is about 2–3 nm[5, 9, 11]. The larger space between layers is more helpful for intercalation of PP[11]. The uniform dispersion of clay in matrix is thought to be a key role in nanocomposite preparation. Since PP has a strong repellency to water due to its non-polar molecule and the montmorillonite is a polar material which has a strong absorption of water, to improve compatibility between MMT and PP matrix is very important to obtain the uniform dispersion of montmorillonite[13]. It is well-known that two methods are usually adopted to improve the compatibility: one is to increase non-polarity of MMT by organic modification treatment[8, 9, 13], and the other is to introduce the compatibilizer containing amphiphatic macromolecules, *e.g.* maleic-anhydride-grafted PP (PP-*g*-MA), for enhancing the compatibility between PP and MMT[4, 5, 7, 13, 14]. Moreover, the preparation method is also an important factor to affect the dispersion of montmorillonite in PP. Up to now, the PP/MMT nanocomposites with exfoliated-MMT structure prepared through *in situ* polymerization and solution blending have been reported[15–19], but these methods are not environment friendly because they need to exhaust large amount of expensive, noxious and unrecoverable solvents. Recently, some researches concerning preparations and properties of PP/MMT nanocomposites by using supercritical CO_2 ($ScCO_2$) technique have been conducted[20–23]. Because of its gas-like diffusivity and liquid-like density which allow replacing in the supercritical phase, $ScCO_2$ can be used as a green processing solvent or plasticizer during polymer melt-blending, and can be used to further improve clay exfoliation in matrix[21, 22]. Although the morphology and the mechanical properties of PP/MMT nanocomposites prepared through melt blending are not better than those by *in situ* polymerization, solution blending or $ScCO_2$, melt blending is still a main and common technique to prepare PP/clay nanocomposites due to its low cost, environment friendliness and convenience[2, 18]. Many efforts have been made to improve the structure, morphology and properties of PP/PP-*g*-MA/MMT nanocomposites[4–14].

Cruz *et al.*[4] entailed the optimization of experimental variables (pressure, temperature, processing time, feed position, *etc*.) of polypropylene and polyethylene films with nanoparticles, and found that the feed position of the nanoparticles in the twin-screw extruder is of vital importance in obtaining an exfoliated film. Sharma *et al.*[5] studied the influences of clay content and different MA-*g*-PP on PP/clay nanocomposites prepared by melt blending technique and found that the typical intercalated and exfoliated structure could lead to a significant increase in the tensile modulus. Ladhari *et al.*[6] prepared polypropylene nanocomposites with two MA-*g*-PP compatibilizers through two-stage processing in a twin-screw extruder, and pointed out that both the absorption rate of moisture and the maximum moisture content increase with the increase of nanoclay content, owing to the hydrophilic nature of the nanoclay and the compatibilizer. Hambir *et al.*[24] prepared PP/clay nanocomposites using different PP, compatibilizers and organically modified clays, and emphasized that the increase in storage modulus is related to the compatibilizer. Marchant *et al.*[13] investigated the structure of PP nanocomposites with different maleated polypropylene compatibilizers prepared by melt-mixing, and noted that the molar ratio of functional group to compatibilizer chain seems a more valid parameter for ranking compatibilizer effectiveness than the acid number.

It is known that isotactic polypropylene is used to prepare polypropylene/MMT nanocomposites, however ethylene/propylene-random-copolymer (PPR) in which the ethylene content is less than 5%, is rarely adopted. PPR is endowed with better stretch flexility and impact resistance as compared with isotactic polypropylene because of the existence of ethylene-propylene rubber component, and it is usually used for packing films. As a few MMT content can improve the properties of polypropylene, especially the gas barrier characteristics of filled polypropylene[7], therefore, it is interesting to study the interplay behavior of PPR with MMT for extending the shelf life of the packaged goods. The purpose of this article is to study the influences of compatibilizers on the dispersion of organically modified montmorillonite (OMMT), composite morphology, thermal behavior and tensile property of PPR/OMMT nanocomposites. In addition, the influence of clay content will be discussed too.

EXPERIMENTAL

Materials

A commercial polypropylene, PPC0723 (ethylene/propylene-random-copolymer with ethylene content of 3.0 wt% and MFI of 7 g/10min at 230°C/2.16 kg) was supplied by Dushanzi Petrochemical Co., China. The grade of OMMT used was Nanomer I.31PS (Nanocor Inc.) purchased from Beijing East-West Chemical Technology LTD, China. The clay was modified using the amino propyl triethoxysilane and octadecylamine, and its cationic exchange capacity was 145 meq/100 g clay. Four kinds of compatibilizers were used, and their data are listed in Table 1.

Table 1. Characteristics of compatibilizers

Sample code	Chemical formula name	Maleic anhydride content (wt%)	MFI (g/10min at 230°C/2.16 kg)	M_w	Molecular weight distribution	Supplier
A	Isotactic homopolypropylene (*i*PP)-graft-maleic anhydride	0.90	160–180	147306	2.5	Ningbo Nengzhiguang New Materials Technology Co., Ltd
B	Block copolymer of propylene (PP-B)-graft-maleic anhydride	0.90	120	136688	4.9	Chenguang Research Institute of Chemical Industry
C	Isotactic homopolypropylene (*i*PP)-graft-maleic anhydride	0.55	30–60	175786	3.3	Nanjing Deba Chemical Co. Ltd (NDC)
D	Ethylene-octene copolymer (POE)-graft-maleic anhydride	0.90	0.5–2.5[a]	201308	5.1	Nanjing Deba Chemical Co. Ltd (NDC)

[a] MFI (g/10min at 190°C/2.16 kg)

Preparation of PPR/OMMT Nanocomposites

The two-stage extrusion method was used to prepare PPR/OMMT nanocomposite on a co-rotating twin-screw extruder (PRISM TSE 16, UK) with a diameter of 16 mm and length-to-diameter ratio of 25. The temperature profile (from feeding to die) used was 160°C, 165°C, 165°C, 170°C and 170°C, and the screw rotation speed was 12 r/min. The PP masterbatches containing 25 wt% OMMT were prepared in the first extrusion. Then, the nanocomposites with desired OMMT contents were prepared in the second extrusion. The compositions of PPR/OMMT nanocomposites are listed in Table 2. The compatibilizer/OMMT mass ratio in all composites was 1.5. The effects of various compatibilizers were investigated when the content of OMMT was fixed at 2 wt% of total mass. The OMMT content ranged from 0.5 wt% to 4.0 wt% when the compatibilizer B was used.

Table 2. Compositions of the PPR/OMMT nanocomposites

Sample code	Compatibilizer	Compostion (PPR/compatibilizer/OMMT) (wt%)
PPR	–	100/0/0
A-2	A	95.0/3.0/2.0
B-2	B	95.0/3.0/2.0
C-2	C	95.0/3.0/2.0
D-2	D	95.0/3.0/2.0
B-0.5	B	98.75/0.75/0.5
B-1		97.5/1.5/1.0
B-3		92.5/4.5/3.0
B-4		90.0/6.0/4.0

Disks with a thickness of 1.0 mm were prepared by compression molding at 190°C for various measurements. The compress pressure used was about 15 MPa.

Characterization

XRD

The X-ray diffraction (XRD) measurements were conducted on a Rigaku D/Max 2550PC apparatus (Rigaku Mechatronics Co. Ltd, Japan) equipped with an incident X-ray of Cu Kα. The operating condition of the X-ray source was set at a voltage of 40 kV and a current of 100 mA. A step of 0.02° was adopted in range of 2θ from 0.5° to 40°. The original OMMT was tested in powder.

DSC

The thermal behavior of PPR/OMMT nanocomposites was measured on a differential scanning calorimeter (DSC Q100, TA Instruments Corporation, USA). The samples were first heated from 40°C to 200°C at 10 K/min, and then kept at 200°C for 5 min to remove the thermal history. Next, they were cooled down to 40°C at 10 K/min, and subsequently were reheated to 200°C at 10 K/min to record the melting traces. All tests were performed in N_2 atmosphere. The endotherm peak temperature on the second heating trace was denoted as the melting temperature (T_m). The crystallinity (X_c) of the samples was calculated using Eq. (1), assuming that the PPR matrix only contains 97 wt% of crystallizable PP. The fusion enthalpy of 100% ($\Delta H_{m100\%}$) PP crystal used were 165 J/g[14].

$$X_c(\%) = \frac{\Delta H_m}{(\Delta H_{m100\%}^{PP} \times \varphi_{PP})} \times 100 \quad (1)$$

in which, ΔH_m is the melting enthalpy of the samples. φ_{PP} is the mass percentage of PP in the nanocomposites.

TEM

The samples were cut to ultra-thin films by an ultra-microtome (Reichert-Jung F4-CD, Rigaku Mechatronics Co. Ltd, Japan). The ultra-thin films were observed to examine the dispersion of the clay in nanocomposites on a transmission electron microscope (TEM, JEM-1200EX, Japan) with an accelerating voltage of 120 kV.

Tensile properties

Tensile properties of the nanocomposites were tested using a Universal tester (Sans CMT4204, MTS System Co., LTD., China) with extensometer according to GB/T 1040. The bars were prepared by cutting samples from the middle sheets. A load cell of 2 kN was used in the experiments. A stretching speed of 50 mm/min was applied for all tests. For each sheet an average of five measurements was adopted.

RESULTS AND DISCUSSION

Effect of Different Compatibilizers on the Microstructure of Nanocomposites

Figure 1 gives the XRD patterns of PPR/OMMT nanocomposites with different compatibilizers. It is seen there the diffraction peaks appear at 2θ angles ranging from 0.5° to 7.5° for nanocomposites indicating the dispersion states of the nano-layers in matrix. According to Bragg's Law, the interplanar distance (d_{001}) can be obtained from the diffraction angle (θ) and the wave length of the incidental radiation (λ).

$$d_{001} = \frac{\lambda}{2\sin\theta} \quad (2)$$

in which, λ is a constant of 0.154 nm.

As shown in Fig. 1, the diffraction peaks for original montmorillonite and composites appearing at different angles indicate the different effects of various compatibilizers on the intercalation of clay. The compatibilizer molecule contains maleic anhydride cations which could react with hydroxyl groups at the edges of clay layers. The reaction could further reduce the interlayer attraction and improve the compatibility between PPR and organoclay, and ultimately enhance the intercalation of PPR into interlayers of clay.

The original montmorillonite presents a diffraction peak at about 4°, corresponding to an interlayer spacing of 2.22 nm. Compared with the original montmorillonite, all the diffraction peaks of the four composites shift towards lower angle and range from 2.2° to 3.2°, indicating that the formation of intercalated structure of clay in the four composites during extrusion. These results are in accordance with previous reports for PP-clay nanocomposites[5–11, 25].

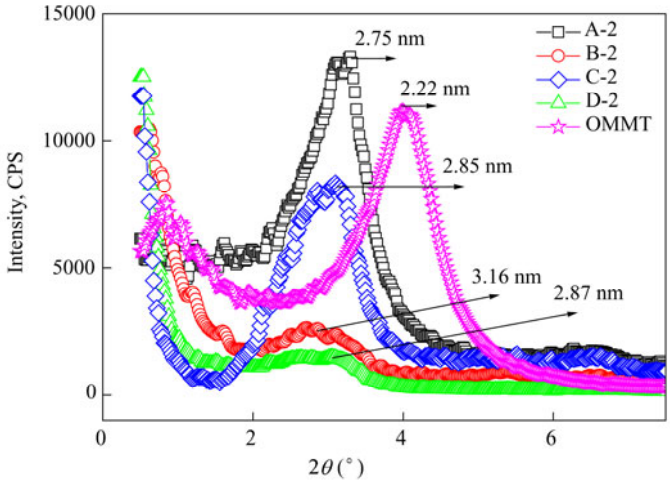

Fig. 1 XRD patterns of PPR/OMMT nanocomposites with different compatibilizers

MA groups in compatibilizers interact with alkyl-ammonium groups in OMMT and help PPR chains to penetrate into clay interlayer more easily. The differences in diffraction intensity among different nanocomposites demonstrate clearly the influences of compatibilizers' grafted groups on the interactions between OMMT and compatibilizers and the compatibilities between OMMT and PPR matrix, allowing compatibilizers and PPR molecular chains to access between platelets of the clay. The content of the intercalated clay layers with a given spacing usually is proportional to the area of the corresponding diffraction peak, while the exfoliated structure of clay does not display any peaks in its XRD pattern[26]. So the position and the intensity of diffraction peaks can exhibit the interaction strength between compatibilizer and OMMT layers and the interface compatibility between compatibilizer and PPR matrix respectively. From Fig. 1, it can be found that the interaction capability of compatibizer B with OMMT layers might be the strongest among the four compatibilizers due to its lowest 2θ value, and those of compatibilizer C and D are similar and all slightly stronger than that of compatibilizer A due to their lower and similar 2θ positions. Except the one with compatibilizer A, the diffraction peaks of other nanocomposites significantly decreased, indicating good intercalation of the clay in the PPR matrix. The nanocomposite with compatibilizer A exhibits the strongest diffraction peak which is even higher than that of the original clay, revealing that the thickness of clay interlayer is the biggest among the four nanocomposites and the interface compatibility between compatibilizer A and PPR matrix maybe is the weakest in the four compatibilizers. The interface compatibilities of compatibizer B and D with PPR matrix are similar and all better than compatibizer C due to their similar and lower diffraction peak altitudes.

Due to the interlayer spacing in composites ranging from 2.75 nm to 3.16 nm, the XRD results reveal that the compatibility effect of compatibilizer B is better than other three compatibilizers. In addition, since it has been well documented that the perfect exfoliated structure of clay in polymeric matrix would usually lead to the disappearance of the XRD peak[4, 26], there possibly exist some clays with exfoliated structure in the composites with compatibilizer B or D due to the rather weak diffraction peaks of clay.

Although the XRD results reveal some possible changes of clay structure in PPR matrix, it is necessary to find the convincing and direct proof on the intercalation of clay. Figure 2 presents the TEM micrograph of

PPR/OMMT nanocomposites with different compatibilizers. It is seen that the dispersions of clay in the four composites are all uniform, but the modalities of OMMT are very different. Table 3 shows the differences of OMMT dispersions among the PPR/OMMT nanocomposites with different compatibilizers, which result from the statistics of length, thickness and shape of clay obtained from TEM results. As shown in the inset of Fig. 2(b), the composite with compatibilizer B presents much better dispersion than others and the dispersion dimension of OMMT is the smallest among the four composites. The percentage of clay particles with their length less than 0.1 μm is about 88%. This reveals that due to its wide molecular weight distribution (MWD), low MFI and the low M_w in the four compatibilizers (as shown Table 1), compatibilizer B has the best compatibility with PPR matrix that makes PPR molecular chains inserting into the clay layers more easily than other compatibilizers and the interlayer distances of the clays being mostly extended[3].

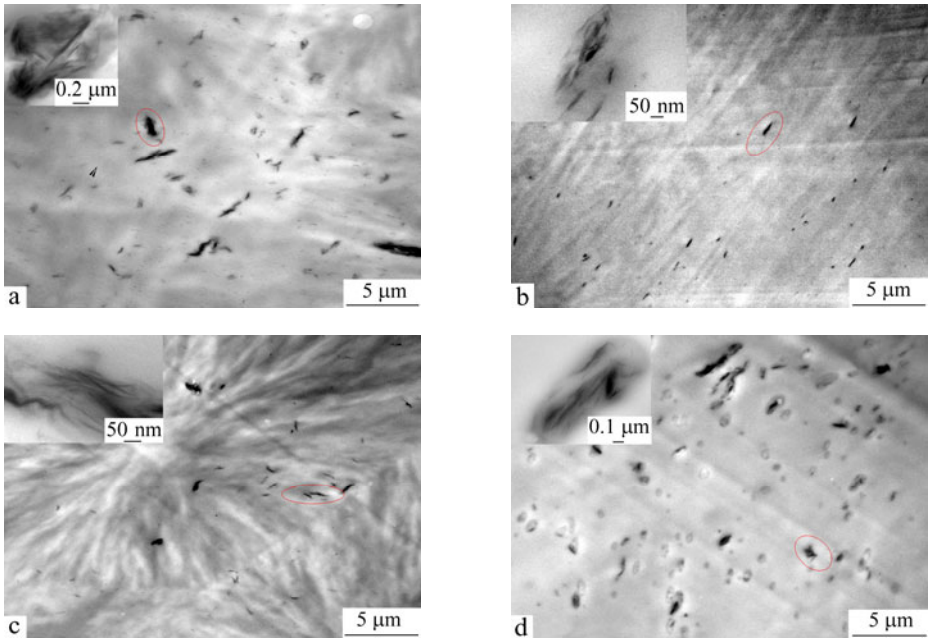

Fig. 2 TEM micrographs of PPR/OMMT nanocomposites with different compatibilizers: (a) A-2, (b) B-2, (c) C-2 and (d) D-2

Table 3. TEM statistics of length, thickness and morphological characteristics of dispersions of OMMT in the PPR/OMMT nanocomposites with different compatibilizers

Sample code	Length	Thickness				Shape
	< 1 μm (%)	< 0.1 μm (%)	< 0.2 μm (%)	< 0.3 μm (%)	< 0.5 μm (%)	
A-2	63.4	7.1	23.8	52.4	73.8	Strip
B-2	87.8	48.6	82.9	88.6	97.1	Strip
C-2	80.5	32.4	70.6	94.1	94.1	Strip
D-2	42.0	0	9.8	29.5	65.6	Ellipse

The OMMT particle dimension of the composite with compatibilizer C is smaller than that with A, which is in accordance with the XRD results. It could be supposed that the strengthened interaction between the clay and compatibilizer C induced more clay layers exfoliated from the stacked structure. The clay dispersion dimension of the composite with compatibilizer D is the largest among the four samples, while the intensity of its diffraction peak is the weakest, implying that there are more exfoliated structures and larger interlayer distance of clay in the composite with compatibilizer D. Moreover, its shape is ellipse, but others are all strip. Figure 2(d) also exhibits that the clays in the composite with compatibilizer D appear more uniform and more exfoliated than those in the other samples, although they are still partly exfoliated and intercalated. As reported

previously[27–31], due to the vast difference in viscosity and incompatibility between POE-*g*-MA and PPR matrix, the clay was almost dispersed first in the POE-*g*-MA phase, revealing that the viscosity difference between compatibilizer and matrix is the key factor of clay dispersion location and modality when compatibilizer and matrix are incompatible. These results were different from the samples with PP-*g*-MA, while the results are similar to the other studies on the PP-clay nanocomposites[32, 33].

As indicated by XRD results, compatibilizer B can remarkably enhance the interlayer spacing (from 2.22 nm to 3.16 nm) and presents the best compatibility among the four compatibilizers. The interlayer spacings of the clays in the composites with compatibilizer D and C are 2.87 and 2.85 nm respectively, indicating that the compatibility effects of compatibilizer D and C are similar. Furthermore, the interlayer spacing in the nanocomposite with compatibilizer A is about 2.75 nm and slightly smaller than that with compatibilizer D and C. According to the above analysis, it is suggested that the compatibility effect of the compatibilizer seems to be related to the MFI, Mw and MWD when compatibilizer and matrix have a good compatibility, and the suitable MFI, Mw and MWD of the compatibilizer would be more propitious to insert interaction between PPR and clay.

Since the compatibility effect of compatibilizer B on PPR/OMMT nanocomposite is better than that of the other compatibilizers, it is necessary to explore the effect of OMMT loadings on its structures. Figures 3 and 4 give the XRD patterns and TEM micrographs of PPR/OMMT/compatibilizer B nanocomposites with different OMMT contents, respectively. The XRD results reveal that all diffraction peaks of the composites shift towards lower angles compared with that of the original OMMT, indicating that the introduction of compatibilizer B has increased the interlayer distance from 2.22 nm to 3.23 nm. When the OMMT content is 0.5 wt%, the diffraction peak appears at 2θ of 2.64°, being the lowest among the five composites. With the increase of OMMT content, the diffraction peak of clay slightly shifts towards higher angles and becomes stronger and narrower, indicating that the dependence of intercalation of clay on the OMMT content. According to their interlayer spacing values, the intercalation effects of the composites containing 0.5 wt% and 2 wt% OMMT are similar and seem stronger than those of the other samples. As Fig. 3 shows, a sharp diffraction peak appears between 2θ value of 0.5° and 2° which is related to improved clay layers, while the intensity of the peak decreases with OMMT content addition except for sample B-0.5. These differences of diffraction peak intensity among various samples reveal clearly the influence of clay content on the interaction between clay and PPR matrix. The intensity of diffraction peaks for B-0.5 and B-2 becomes stronger than that of original OMMT, implying that the concentration of sole clay interlayer increases[14, 34]. The same phenomenon is also seen clearly in Fig. 4. In Fig. 4, although all the samples present relatively uniform dispersion of clay, clay distributions of the samples containing 0.5 wt% and 2.0 wt% OMMT appear much better, and the dimensions and modalities of OMMT in them are smaller and more exfoliated than those of other samples. No obvious change in the dimension or shape of OMMT could be found when the OMMT content increases from 3.0 wt% to 4.0 wt%.

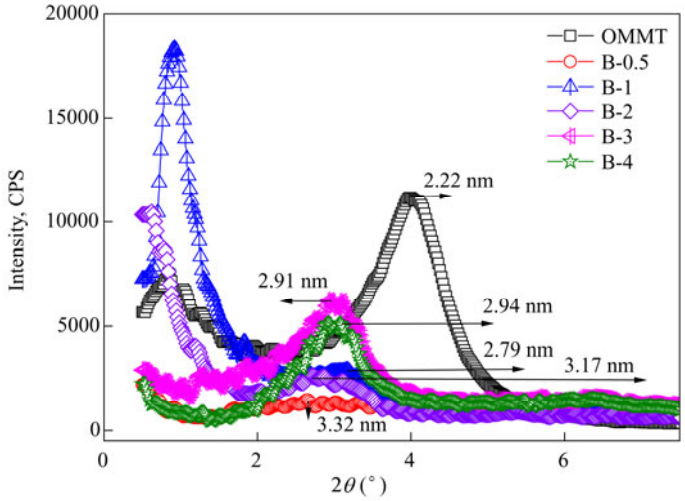

Fig. 3 XRD patterns of PPR/OMMT nanocomposites with different OMMT contents

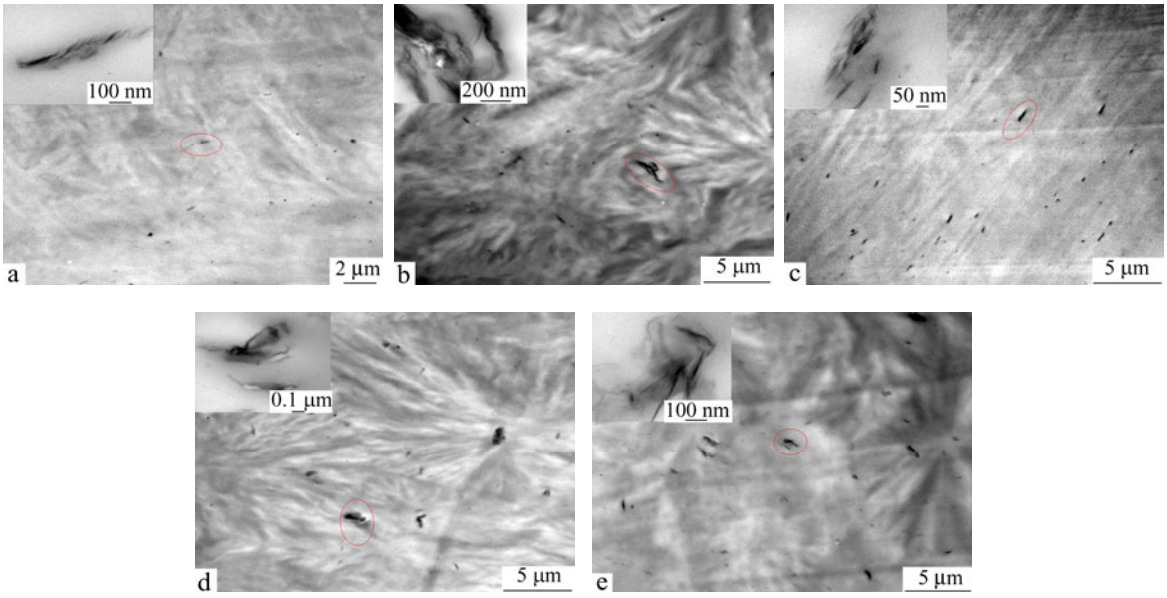

Fig. 4 TEM micrographs of PPR/OMMT nanocomposites with different OMMT contents: (a) B-0.5, (b) B-1, (c) B-2, (d) B-3 and (e) B-4

These results indicate that there is no significant change in interlayer distance and dispersion modality of clay when the clay content increases from 0.5 wt% to 4.0 wt%. In all samples the clay is intercalated and partly exfoliated.

The Crystallization Behavior of the Nanocomposites

Since the addition of compatibilizer can affect the dispersion of clay in composites, it is necessary to explore the effect of compatibilizer on the crystallization of nanocomposites. Figure 5 gives the exotherms and endotherms of PPR/OMMT nanocomposites with different compatibilizers. The relative crystallization data are listed in Table 4.

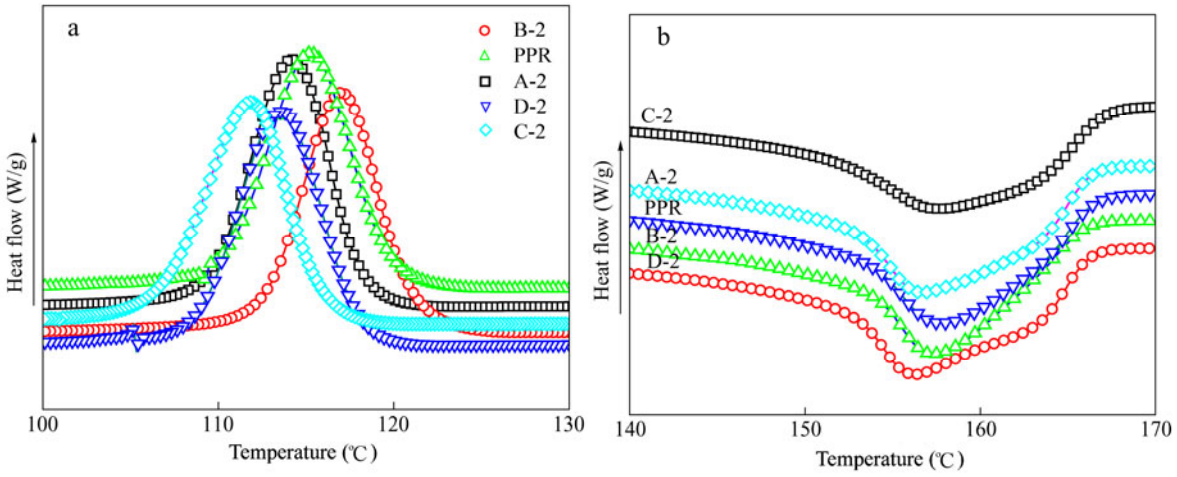

Fig. 5 Exotherms (a) and endotherms (b) of PPR/OMMT nanocomposites with different compatibilizers

Table 4. DSC results of PPR/OMMT nanocomposites with different compatibilizers

Sample code	Compatibilizer	OMMT addition (%)	DSC				
			$T_{m,onset}$ (°C)	T_m (°C)	$T_{c,onset}$ (°C)	T_c (%)	X_c (%)
PPR	–	0	151.1	157.8	119.7	115.3	55.2
A-2	A	2	143.7	156.9	118.1	114.2	50.7
B-2	B	2	151.4	157.3	121.1	117.0	56.7
C-2	C	2	149.3	158.0	120.6	112.5	56.5
D-2	D	2	150.6	156.3	118.0	113.6	55.1

As seen from the data, it is obvious that different compatibilizers have distinct effects on the crystallization of PPR/OMMT composites. The introduction of compatibilizer B leads to slight increases in crystallizing onset temperatures ($T_{c,onset}$), T_c and X_c of PPR matrix. On the contrary, both the composites with compatibilizer C and D present a decrease of T_c compared with neat PPR matrix, but the composite with compatibilizer C shows a slight increase in X_c, and the one with compatibilizer D is similar with PPR. Moreover, the addition of compatibilizer A leads to an evident decrease in X_m. From the above results, it could be inferred that compatibilizer B can remarkably enhance the nucleation effect of clay layers on PPR crystallization, and compatibilizer A has the contrary effect. According to the above clay distribution results, the variations of $T_{c,onset}$ and T_c in PPR/clay composites with different compatibilizers were associated with the exfoliation and intercalation degree of clay layers, and the highest increase in $T_{c,onset}$ and T_c for PPR crystallization corresponded to the greatest degree of clay delaminated structure in composite B-2. However, the melting onset temperatures ($T_{m,onset}$) for these composites seem not significantly varied except for sample A-2 having an evidently lower $T_{m,onset}$ compared with that of neat PPR matrix. In particular, the composite with compatibilizer A presents a much broader melting peak than other samples, and a decrease of about 8% in crystallinity could be found compared with neat PPR matrix, which maybe is due to the high thickness of clay layers in composite A-2 that induces the decrease of clay nucleation and the formation of more irregular and bigger PP spherulites than those of PPR matrix, that decreases crystal perfection of PP crystallization. Except for compatibilizer A, other compatibilizers show little effect on their nanocomposites' T_m and crystallinity, suggesting that even the compatibilizers can affect the crystallization and melting behavior, they still have little effect on the crystallinity of composites. The results are in agreement with the previous studies[14, 32, 33]. Since the melting temperature is mainly related to the lamellae thickness, and the width of melting peak presents the difference in degree of crystal perfection, the lamellae thickness in the composites might be independent of the compatibilizers although the compatibilizers could lead to some changes in nucleation ability and crystal perfection among different composites, suggesting that the crystalline structure of PPR was hardly affected by the added compatibilizers and clay.

Table 5. DSC properties of PPR/OMMT nanocomposites with different OMMT loadings

Sample code	Compatibilizer	OMMT addition (%)	DSC					
			$T_{m,\beta}$ (°C)	$T_{m,onset}$ (°C)	T_m (°C)	$T_{c,onset}$ (°C)	T_c (°C)	X_m (%)
PPR	–	0	–	151.1	157.8	119.7	115.3	55.2
B-0.5		0.5	146.2	152.2	158.7	120.8	116.6	56.2
B-1		1	142.9	150.8	157.1	118.3	114.4	56.4
B-2	B	2	144.9	151.4	157.3	121.1	117.0	56.7
B-3		3	142.9	150.8	156.6	119.0	115.2	55.2
B-4		4	142.7	150.3	156.5	118.5	114.9	53.3

Figure 6 gives the exotherms and endotherms of PPR/OMMT nanocomposites with different OMMT and compatibilizer B loadings, and Table 5 shows the corresponding DSC results. When the OMMT content increases from 0.5 wt% to 4.0 wt%, a slight increase in the crystallinity could be found except for sample B-4 and a little β-PP crystal could be found. Moreover, it is found that the composite with OMMT content of 2 wt% seems to appear some differences in T_m and T_c, that being agreed with the other investigators for PP-clay

nanocomposites[14, 32, 33]. The above results imply that the nucleation effect of clay layers on PPR crystallization is remarkably promoted when the OMMT content is 2 wt%.

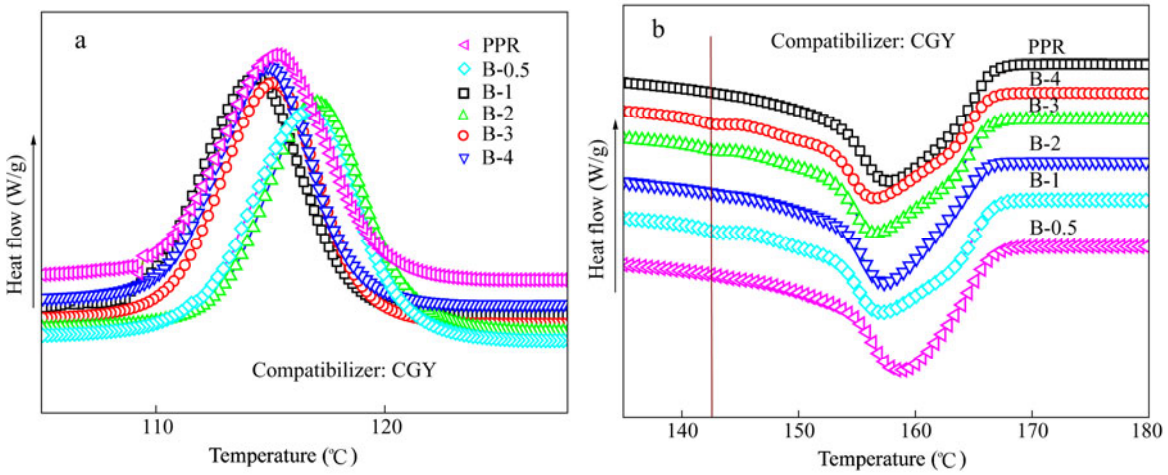

Fig. 6 Exotherms and endotherms of PPR/OMMT nanocomposites with different OMMT contents

The Tensile Properties

Table 6 lists the tensile properties of PPR/ OMMT with different compatibilizers. The mechanical properties of nanocomposites depend on many factors such as the aspect ratio of clay, the dispersion degree of clay in the matrix, the adhesion at clay-matrix interface, etc. As seen in Table 6, for all composites, their tensile yield strengths are similar to that of the neat PPR matrix, but their breaking strength and breaking elongation remarkably decrease. These results indicate that not only the interfacial strength between clay and PPR matrix but also the intermolecular interaction between PPR chains decreases greatly due to the addition of inorganic clay into PPR matrix, although the compatibilizers can improve the dispersion of OMMT in PPR matrix, especially for samples with compatibilizer C and D. When the compatibilizers improve the interfacial adhesion between fillers (clay) and polymer matrix, the polar functional groups in the compatibilizer would bind with the surface of clay and the polymer backbone of the compatibilizer would mix well with the matrix. As reported in literatures[33–35], the interaction between clay and matrix decreased with the decrease of compatibilizer content and so did the tensile breaking properties. In present paper, the compatibilizer/OMMT mass ratio in all composites is 1.5/1, that is very low compared with that in the previous reports. According to the above results, the compatibilizer with low M_w and big MFI is obviously more beneficial to improve the adhesion strength at clay-PPR matrix interface.

Table 6. Tensile properties of PPR/OMMT with different compatibilizers

Sample code	Compatibilizer	OMMT addition (%)	Tensile yield strength (MPa)	Breaking strength (MPa)	Breaking enlongation (%)	Young's Modulus E (MPa)
PPR	–	0	35 ± 0.4	46 ± 0.9	1412 ± 0.3	287 ± 14.3
A-2	A	2	34 ± 0.2	28 ± 0.8	761 ± 0.9	183 ± 9.2
B-2	B	2	35 ± 0.3	27 ± 1.3	738 ± 0.5	271 ± 13.5
C-2	C	2	33 ± 0.3	23 ± 0.3	393 ± 0.4	348 ± 17.4
D-2	D	2	34 ± 0.2	25 ± 1.0	285 ± 0.7	279 ± 13.9

The Young's modulus of the composite with compatibilizer A decreases by about 36% compared with neat PPR matrix due to the decrease of its crystallization perfection and the dispersion of nano-clay (as shown in Fig. 1 and Table 3). The XRD diffraction peak intensity of clay at 2θ of 2°–5° in the sample with compatibilizer A is the highest among the four samples, implying that the accumulation thickness of clay lamellae is the

highest. The thicker the clay lamellae in composite is, the weaker the adhesion strength between clay and PPR matrix is. Additionally, the crystallinity of the composite with compatibilizer A decreases by about 8% compared with neat PPR matrix, indicating that the crystallization perfection in this sample decreases accordingly. On the other hand, the Young's modulus of the composite with compatibilizer C increases by about 21% only due to its better crystallization perfection (sees Fig. 5 and Table 4). The $T_{c,onset}$, and T_c of the sample with compatibilizer C are the lowest among the five samples and its X_c also increases slightly, indicating that its crystallization speed is the lowest and its crystallization perfection improves slightly. This reveals that the compatibilizer with large M_w and wide MWD is of great benefit to increasing the Young's modulus of composites. Based on the above results, compatibilizer B is considered as the optimized one from the overall merit.

Table 7 lists the tensile properties of PPR/OMMT with different OMMT and compatibilizer B contents. It is seen that there exists a trend of decrease in the breaking strength and elongation for the composites when the OMMT loading increase from 0.5 wt% to 3.0 wt%. This indicates that the interfacial strength between clay and PPR matrix decreases gradually with the OMMT content increasing. But the breaking strength and breaking elongation of the samples with 4.0 wt% clay content increase conversely. The phenomena might be related to the dispersion of clay in the samples. According to the clay distribution as shown in Fig. 3, the sample B-4 has a lowest XRD diffraction peak at about 0.5° among five samples, which is the same as sample B-0.5, implying that the concentration of sole clay interlayer is also the lowest and makes its deforming resistance increased. Furthermore, the Young's modulus of sample B-0.5 increases by about 15% and that of sample B-1 decreases by 43% compared with neat PPR matrix also due to the different dispersions of clay in the composites. Although the interplanar distance of the nanocomposites with different OMMT contents at 2θ of 2° and 4° is similar, but the intensity of diffraction peak located at about 0.5°–2° is quite different, especially for sample B-1. The intensity of diffraction peak of sample B-1 at 2θ value of 0.5° and 2.0° is the highest among the five samples and even stronger than that of original OMMT, implying that the concentration of sole clay interlayer is the highest and induces the decrease of adhesion strength at clay-PPR matrix interface.

Table 7. Tensile properties of PPR/OMMT with different OMMT loadings

Sample code	Compatibilizer	OMMT addition (%)	Tensile yield strength (MPa)	Breaking strength (MPa)	Breaking enlongation (%)	Young's Modulus E (MPa)
PPR	–	0	35 ± 0.4	46 ± 0.9	1412 ± 0.3	287 ±14.3
B-0.5		0.5	34 ±0.2	41 ± 1.7	1310 ± 0.4	330 ±16.5
B-1		1	34 ±0.2	35 ± 1.1	1065 ± 0.5	163 ±8.2
B-2	B	2	35 ±0.3	27 ± 1.7	738 ± 0.5	271 ± 13.5
B-3		3	32 ±0.5	27 ± 2.0	737 ± 0.8	242 ± 12.1
B-4		4	33 ±0.1	34 ± 1.1	1032 ± 0.5	198 ± 9.9

Compared with neat PPR matrix, the tensile yield strength of the composites with different OMMT and compatibilizer B loadings also decrease more or less, but the tensile yield strength and Young's modulus of sample B-2 vary little. Therefore, it is necessary to maintain a suitable balance between the toughness and stiffness of nanocomposites through OMMT contents. In view of the above analysis, it is proposed that 2.0 wt% OMMT was an optimum concentration for the affinity of PPR molecules and clay layers in composites, which is consistent with the thermal analysis results and the morphology observation of clay layers in sample B-2.

CONCLUSIONS

The PPR/clay nanocomposites with different maleic anhydride graft polymers as compatibilizer have been prepared by a two-stage melt-mixing procedure. So far as the dispersion of organo-modified clay is concerned, there exist intercalated and partly exfoliated structures, and the spaces between nano-clayers are expanded evidently by the compatibilizers, especially by compatibilizer B. The compatibilizer type and the OMMT

loadings have little effect on T_m and a slight effect on T_c of the composites. Only compatibilizer B could lead to the obvious increases in the crystallinity and T_c of the composite in case of OMMT content being 2 wt%. Moreover, the increase of compatibilizer and OMMT loadings can decrease the breaking strength, breaking elongation, tensile yield strength and Young's modulus of their composites more or less, especially for breaking elongation. However, compatibilizer C increases distinctly the Young's modulus of the composite, and compatibilizer B demonstrates the best compatibility. It is suggested that the most suitable content of OMMT is 2 wt% with compatibilizer B.

REFERENCES

1 Ramadan, A.R., Esawi, A.M.K. and Gawad, A.A., Appl. Clay Sci., 2010, 47: 196
2 Pfaendner, R., Polym. Degrad. Stab., 2010, 95: 369
3 Perrin-Sarazin, F., Ton-That, M.T., Bureau, M.N. and Denault, J., Polymer, 2005, 46: 11624
4 Abreu, D.A.P.d., Losada, P.P., Angulo, I. and Cruz, J.M., Eur. Polym. J., 2007, 43: 2229
5 Sharma, S.K., Nema, A.K. and Nayak, S.K., J. Appl. Polym. Sci., 2010, 115: 3463
6 Ladhari, A., Daly H.B., Belhadjsalah, H., Cole, K.C. and Denault, J., Polym. Degrad. Stab., 2010, 95: 429
7 Mittal, V., J. Appl. Polym. Sci., 2008, 107: 1350
8 Osman, M.A., Mittal, V. and Suter, U.W., Macromol. Chem. Phys., 2007, 208: 68
9 Mittal, V., J. Thermoplast. Compos. Mater., 2007, 20: 575
10 Cauvin, L., Kondo, D., Brieu, M. and Bhatnagar, N., Polym. Test., 2010, 29: 245
11 Dong, Y. and Bhattacharyya, D., Composites Part A, 2008, 39: 1177
12 Martin, Z., Jimenez, I., Gomez, M.A., Ade, H.W., Kilcoyne, D.A. and Hernadez-Cruz, D., J. Phys. Chem. Part B, 2009, 113: 11160
13 Marchant, D. and Jayaraman, K., Ind. Eng. Chem. Res., 2002, 41: 6402
14 Chinellato, A.C., Vidotti, S.E., Hu, G.H. and Pessan, L.A., Compos. Sci. Technol., 2010, 70: 458
15 Ma, J.S., Qi, Z.N., Zhang, S.F., Wang, X., Chen, S.J. and Hu, Y.L., Chem. J. Chin. Univ., 2001, 22: 1767
16 Yuan, X.H., Li, X.H., Zhu, E., Hu, J., Cao, S.S. and Sheng, W.C., Carbohydr. Polym., 2010, 79: 373
17 Baniasadi, H., Ramazani S.A., A. and Nikkhah, S.J., Mater. Des., 2010, 31: 76
18 Yang, K.F., Huang, Y.J. and Dong, J.Y., Polymer, 2007, 48: 6254
19 Zhao, Y. and Huang, H.X., Polym. Test., 2008, 27: 129
20 Nalawade, S.P., Picchioni, F. and Janssen, L.P.B.M., Prog. Polym. Sci., 2006, 31: 19
21 Nguyen, Q.T. and Baird, D.G., Polymer, 2007, 48: 6923
22 Ma, J., Bilotti, E., Peijs, T. and Darr, J.A., Eur. Polym. J., 2007, 43: 4931
23 Hambir, S., Bulakh, N. and Jog, J.P., Polym. Eng. Sci., 2002, 42: 1800
24 Li, J., Zhou, C.X., Wang, G. and Zhao, D.L., J. Appl. Polym. Sci., 2003, 89: 3609
25 Richard, A.V. and Emmanuel, P.G., Macromolecules, 1997, 30: 8000
26 Kontopoulou, M., Liu, Y.Q., Austin, J.R. and Scott Parent, J., Polymer, 2007, 48: 4520
27 Hong, J.S., Namkung, H., Ahn, K.H., Lee, S.J. and Kim, C., Polymer, 2006, 47: 3967
28 Dharaiya, D.P. and JANA, S.C., J. Polym. Sci. Part B: Polym. Phys., 2005, 43: 3638
29 Chen, B.Q. and Evans, J.R.G., J. Phys. Chem. B., 2004, 108: 14986
30 Zhu, Y., Ma, H.Y., Tong, L.F. and Fang, Z.P., Chinese J. Polym. Sci., 2008, 26(6): 783
31 Zhong, W.X., Qiao, X.Y., Sun, K., Zhang, G.D. and Chen, X.D., J. Appl. Polym. Sci., 2006, 99: 2558
32 Lai, S.M., Chen, W.C. and Zhu, X.S., Composites Part A, 2009, 40: 754
33 Kawasumi, M., Hasegawa, N., Kato, M., Usuki, A. and Okada, A., Macromolecules, 1997, 30: 6333